Bioisosterism

International Edition: DOI: 10.1002/anie.201905452
German Edition: DOI: 10.1002/ange.201905452

Inverting Small Molecule–Protein Recognition by the Fluorine *Gauche* Effect: Selectivity Regulated by Multiple H→F Bioisosterism

*Patrick Bentler, Klaus Bergander, Constantin G. Daniliuc, Christian Mück-Lichtenfeld, Ravindra P. Jumde, Anna K. H. Hirsch, and Ryan Gilmour**

Dedicated to Professor François Diederich on the occasion of his retirement

Abstract: *Fluorinated motifs have a venerable history in drug discovery, but as C(sp^3)–F-rich 3D scaffolds appear with increasing frequency, the effect of multiple bioisosteric changes on molecular recognition requires elucidation. Herein we demonstrate that installation of a 1,3,5-stereotriad, in the substrate for a commonly used lipase from Pseudomonas fluorescens does not inhibit recognition, but inverts stereoselectivity. This provides facile access to optically active, stereochemically well-defined organofluorine compounds (up to 98% ee). Whilst orthogonal recognition is observed with fluorine, the trend does not hold for the corresponding chlorinated substrates or mixed halogens. This phenomenon can be placed on a structural basis by considering the stereoelectronic gauche effect inherent to F–C–C–X systems (σ→σ*). Docking reveals that this change in selectivity (H versus F) with a common lipase results from inversion in the orientation of the bound substrate being processed as a consequence of conformation. This contrasts with the stereochemical interpretation of the biogenetic isoprene rule, whereby product divergence from a common starting material is also a consequence of conformation, albeit enforced by two discrete enzymes.*

Arigoni and Eschenmoser's stereochemical interpretation of the biogenetic isoprene rule is synonymous with placing enzyme function on a structural level.[1] Predicated on efficient substrate pre-organisation governed by a specific cyclase (Figure 1), this treatise rationalises the conversion of oxidosqualene to either lanosterol or β-amyrin. Described as the "apotheosis of the isoprene rule" by Cornforth,[2] this interpretation has proven to be expansive and continues to inform and inspire the design of cyclisation cascades for the rapid generation of structural complexity.[3] This study, together with the contemporaneous work from Stork and Burgstahler,[4] nucleates upon an acyclic conformational analysis of oxidosqualene.[5] The manifest selectivity of these two, discrete enzymatic processes is a consequence of (i) minimisation of non-bonding interactions, and (ii) further conformational refinement in the enzyme–substrate ensemble. Whilst the latter is pervasive in enzyme catalysis and ultimately responsible for structural divergence, achieving orthogonal reactivity encoded at the substrate conformation level is comparatively underexplored. This is a logical consequence of enzyme specificity and the need for effective bioisosteres that modulate conformation but do not inhibit recognition.[6]

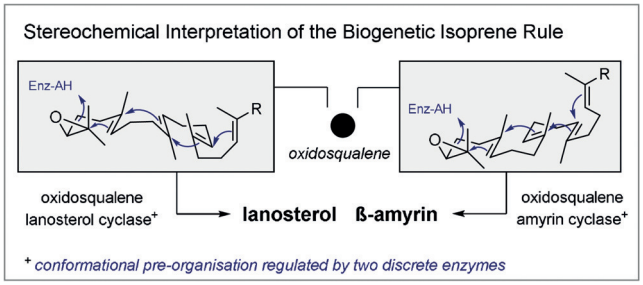

Figure 1. Stereochemical interpretation of the biogenetic isoprene rule.

Multiple hydrogen to fluorine substitution is ideally suited to the task, since this subtle steric modification induces a localised partial charge inversion (C-$H^{\delta+}$ → C-$F^{\delta-}$). This strategy enabling physicochemical modulation[7] also provides a potentially expansive platform to modulate molecular recognition in a manner distinct from the role of fluorine in interrogating enzyme function.[8] The strategic introduction of configurationally defined C(sp^3)–F centres offers an additional degree of versatility in allowing the structural and

[*] Dr. P. Bentler, Dr. K. Bergander, Dr. C. G. Daniliuc, Dr. C. Mück-Lichtenfeld, Prof. Dr. R. Gilmour
Organisch Chemisches Institut
Westfälische Wilhelms-Universität Münster
Corrensstraße 40, 48149 Münster (Germany)
E-mail: ryan.gilmour@uni-muenster.de
Homepage: http://www.uni-muenster.de/Chemie.oc/gilmour/
Dr. R. P. Jumde, Prof. Dr. A. K. H. Hirsch
Helmholtz Institute for Pharmaceutical Research Saarland (HIPS), Helmholtz Centre for Infection Research (HZI), Department of Drug Design and Optimization
University Campus E8.1, 66123 Saarbrücken (Germany)
Prof. Dr. A. K. H. Hirsch
Department of Pharmacy, Saarland University
66123 Saarbrücken (Germany)
Supporting information and the ORCID identification number(s) for the author(s) of this article can be found under https://doi.org/10.1002/anie.201905452.

© 2019 The Authors. Published by Wiley-VCH Verlag GmbH & Co. KGaA. This is an open access article under the terms of the Creative Commons Attribution-NonCommercial-NoDerivs License, which permits use and distribution in any medium, provided the original work is properly cited, the use is non-commercial and no modifications or adaptations are made.

electronic topology to be regulated by stereoelectronic and electrostatic effects.[9]

The stereoelectronic *gauche* effect[10] intrinsic to the 1,2-difluoro motif,[11] together with electrostatic 1,3-repulsion, validate the potential of synergistic fluorine effects and multiple bioisosterism in achieving acyclic conformational control. Consequently, stereochemically complex, fluorine-rich architectures are suited to divert the intrinsic selectivity of a given enzyme, observed with the non-fluorinated case, via two discrete substrate-enzyme ensembles (Figure 2, top).[12]

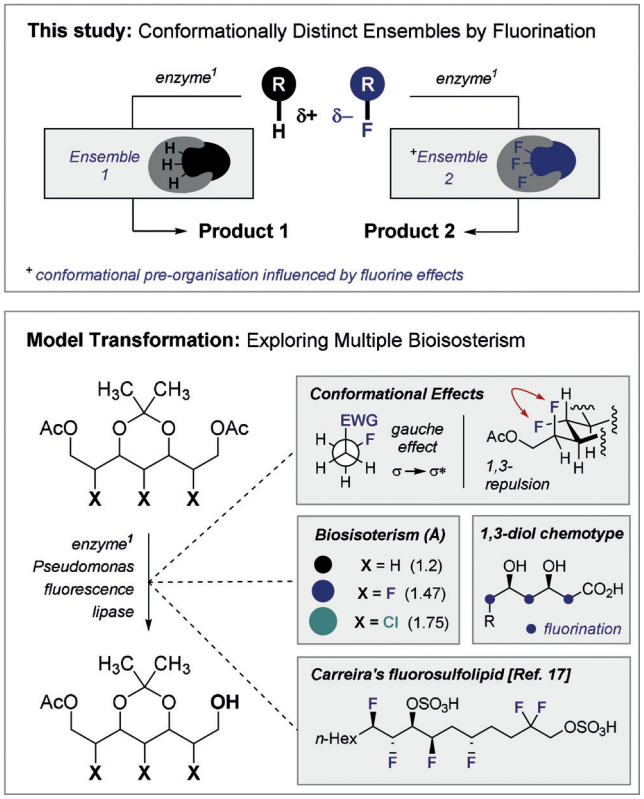

Figure 2. Conceptual framework of this study (EWG: electron withdrawing group).

As a model for this study, the desymmetrisation of a meso-acetate (X = H) utilising lipase from *Pseudomonas fluorescence* was investigated (Figure 2, bottom).[13,14] This scaffold is a convenient platform to interrogate multiple bioisosterism (X = H, F and Cl) as a function of Van der Waals radii, and allows for conformational regulation by virtue of the fluorine *gauche* effect and 1,3-repulsion. The desymmetrisation platform would also provide facile access to stereochemically complex, multiply fluorinated systems in an optically active form.[15] Derivatives of the parent scaffold continue to be produced on an industrial scale for the production of various blockbuster pharmaceuticals such as Lipitor and related statins.[16] Moreover, 1,3-*syn* diols are ubiquitous in polyketides, and construction of the 1,3,5-trifluoro motif is a highlight of Carreira's synthesis of a fluorosulfolipid (Figure 2, bottom).[17]

Initially, the notion of inverting the intrinsic sense of stereoselection by multiple H to F substitution was interrogated by docking studies using LeadIT.[19] To that end, substrates **1** and **2** were docked into the active site of the *Pseudomonas fluorescens* HU380 lipase to establish if the bound topologies showed appreciable differences. This analysis revealed a striking difference in both the orientation and conformation of these closely similar molecules in the active site. The conformation of the bound, fluorinated *meso*-substrate clearly manifested fluorine–ester *gauche* effects, and partial miminisation of 1,3-repulsion (Figure 3a,b. For a computational analysis of unbound **1** and **2**, see the Supporting Information (SI)).

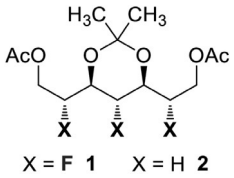

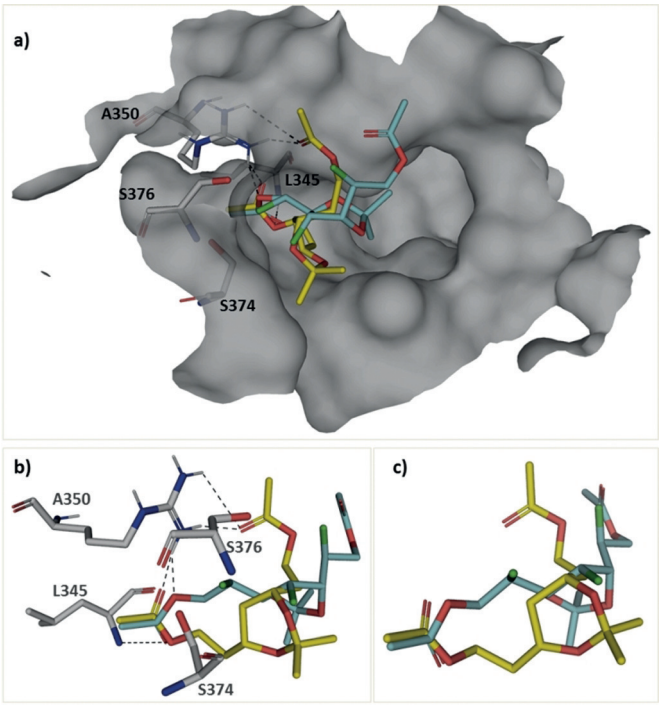

Figure 3. Comparative orientations of the fluorinated and non-fluorinated *meso*-substrates docked in the active site of *Pseudomonas fluorescens* HU380 lipase. a) Fluorinated (1) and non-fluorinated (2) *meso*-acetates with protein surface and their interaction with amino acid residues in the binding pocket. b) Interaction of fluorinated and non-fluorinated *meso*-acetates with important amino acid residues. c) Superimposed fluorinated and non-fluorinated *meso*-acetates. Hydrogen bonds below 3.6 Å are shown as dashed, black lines. Colour code: protein surface: grey; protein skeleton: C: grey; fluorinated *meso*-acetate: C: cyan; non-fluorinated *meso*-acetate: C: yellow; O: red; N: blue; F: green. This figure was generated using PyMOL (Schrödinger).[18]

Most importantly, the effect of fluorine bioisosterism is to reposition the internal carbonyl groups of **1** compared to the non-fluorinated congener **2**, without inhibiting recognition. Whilst the carbonyl groups diverge slightly in their spatial orientation (Figure 3b), both are proximal to the nucleophilic serine residue (S374). This computational analysis thus provided confidence to proceed to experimental validation to establish that ground state changes achieved via molecular

 © 2019 The Authors. Published by Wiley-VCH Verlag GmbH & Co. KGaA, Weinheim

Table 1: Optimisation of the hydrolytic enzymatic desymmetrisation of **1**.[a]

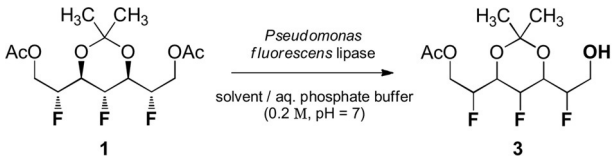

1 **3**

Entry	Solvent	Ratio [*v*/*v*]	Enzyme loading [mg/μmol]	Conversion [%][b]
1	aq. buffer	–	0.3	n.d.
2	aq. buffer/methanol	1:1	0.3	n.d.
3	aq. buffer/ethanol	1:1	0.3	50
4	aq. buffer/isopropanol	1:1	0.3	< 5
5	aq. buffer/acetonitrile	1:1	0.3	< 5
6	aq. buffer/THF	1:1	0.3	< 5
7	aq. buffer/chloroform	1:1	0.3	< 5
8	aq. buffer/DMF	1:1	0.3	> 95
9[c]	**aq. buffer/DMF**	**3:1**	**0.1**	**> 95**

[a] Standard reaction conditions: *meso*-2,4,6-trifluoro-1,3,5,7-tetrahydroxyheptane-1,7-diacetate (**1**) (17 mg, 50 μmol), aq. phosphate buffer (0.2 M)/ co-solvent (1:1 v/v, 10 mL), lipase 15 mg (*Pseudomonas fluorescens*, ≥ 600 U/g immobilised on Immobead 150), ambient temperature, 18 h. [b] Conversion was monitored via GC analysis. [c] **1** (150 μmol), aq. phosphate buffer (0.2 M)/ DMF (3:1 v/v, 20 mL).

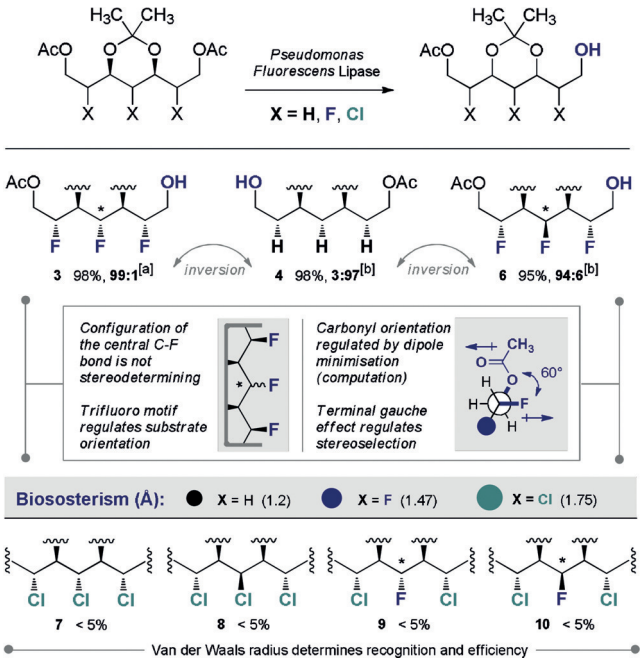

Figure 4. Exploring the effect of F versus H on the selectivity of the transformation. [a] Enantiomeric ratio (*e.r.*) determined by chiral GC analysis. [b] Enantiomeric ratio could not be directly determined by GC or HPLC. Diastereomeric ratio (*d.r.*) determined by converting the alcohol to the Mosher ester and subsequent ^{19}F NMR analysis (see Supporting Information).

editing with fluorine can have significant implications for enzyme function (Figure 3c).

Encouraged by the computational data, the tolerance of the lipase to the 1,3,5-trifluoro motif was explored in the desymmetrisation of meso-substrate **1** (Table 1). This required the identification of conditions that were compatible with both the trifluorinated substrate **1** and the non-fluorinated control (**2**). Full details regarding the stereocontrolled synthesis of the substrates are provided in the Supporting Information. An optimisation process identified a solvent ratio of aq. buffer/DMF (3:1) and an enzyme loading of 0.1 mg μmol^{-1} to be highly effective, resulting in > 95% conversion to the product **3**.

With these optimised conditions, the effect of fluorine introduction on the selectivity of the reaction with lipase from *Pseudomonas fluorescens* was investigated and compared directly to the non-fluorinated analogue (Figure 4, top). Gratifyingly, after 18 h the all-*anti* substrate (**1**) was cleanly processed to alcohol **3** in 98% yield and with exquisite selectivity (99:1 *e.r.*). The key control experiment with the non-fluorinated analogue (**2**) required doubling of the enzyme loading to 0.2 mg μmol^{-1} and stirring in neat aq. phosphate buffer (0.2 M, pH 7) for 112 h. Whilst the reaction proved to be efficient both in terms of yield (**4**, 98%) and selectivity (3:97 *d.r.*, determined by derivatisation to the Mosher ester, see SI), the effect of deleting the fluorine motif was to invert the intrinsic sense of stereoselection. To explore this phenomenon further, the C4 epimer **5** (*anti*,*syn*,*syn*,*anti*, see the SI) was investigated (Figure 4): Again, the sense of selectivity was in line with product **3** and furnished **6** in 95% yield (94:6 *d.r.* determined by derivatisation to the Mosher ester, see SI). As an important set of control substrates, the *tris*-chloro and mixed interhalogen examples were prepared (Figure 4, bottom). In all four cases, < 5% conversion was observed (**7**–**10**) further underscoring the ability of fluorinated arrays to effectively mimic hydrocarbon scaffolds. For completion, the desymmetrisation of the *meso*-diol **11** was also explored and compared with the non-fluorinated counterpart (**12**). Gratifyingly, this compound proved to be crystalline. Structural analysis by single-crystal X-ray diffraction revealed the *gauche* ($\sigma_{C\text{-}H} \rightarrow \sigma_{C\text{-}F}^*$) and 1,3-repulsion effects that were part of the working hypothesis.

Bonini and co-workers have reported that the formation of *ent*-**4** arises from the lipase catalysed transesterification of the *meso*-diol with vinyl acetate (Figure 5, top).[13] However, upon repeating these conditions with the trifluorinated substrate **11** using 20 equiv. of vinyl acetate, only the diacetate (**1**) was isolated. By reducing the equivalents of vinyl acetate it was possible to demonstrate that the selectivity of his process using the fluorinated substrate was inverted, furnishing *ent*-**3** (7:93 *e.r.*).[13] This key experiment thereby illustrates that selectivity is encoded at the substrate level thereby allowing product enantiomers to be generated depending on the starting material (diol versus *bis*-acetate) (Figure 6).

To demonstrate the synthetic utility of the enzymatic desymmetrisation in the generation of optically active, multiply fluorinated systems, the diol chain common to a series of blockbuster HMG-CoA reductase inhibitors was prepared (Figure 7). Synthesis of the drug chemotype analogue common to Lipitor, Cerivastatin, Fluvastatin and Rosuvastatin was achieved by enzymatic desymmetrisation, and subsequent oxidation to the ester (**13**/**14**).[20] Conversion to the azide (**15**/**16**) provides a valuable handle to install a multitude

 © 2019 The Authors. Published by Wiley-VCH Verlag GmbH & Co. KGaA, Weinheim

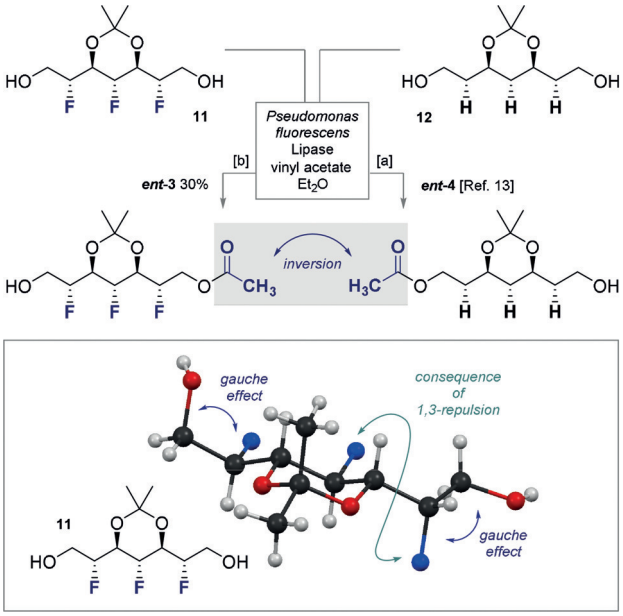

Figure 5. X-ray structural analysis of the *meso*-2,4,6-trifluoro-1,3,5,7-tetrahydroxyheptanol **11**. [a] Ref. [13]: *Meso*-diol **12** (100 µmol), Et_2O (4 mL), *Pseudomonas fluorescens* Lipase (100 mg, 4.0 mass eq.), vinyl acetate (20.0 equiv.), ambient temperature, 18 h. [b] *Meso* diol **11** (100 µmol), Et_2O (4 mL), *Pseudomonas fluorescens* Lipase (50 mg, 2.0 mass eq.), vinyl acetate (2.0 equiv.), ambient temperature, 4 h; 64% recovered starting material **11**.

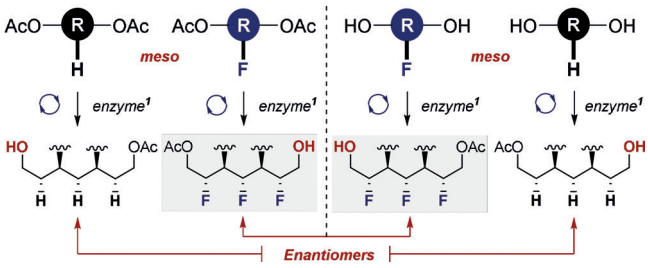

Figure 6. Demonstrating that 1,3,5-trifluorination alters the intrinsic selectivity of catalysis in both directions (hydrolysis and esterification).

of aryl fragments as represented by the triazole (**23**/**24**). Reduction to the amine (**17**/**18**) and subsequent amidation furnished a crystalline derivative (**19**/**20**) thereby allowing the absolute and relative stereochemistry to be unequivocally established by X-ray analysis (Figure 7, inset). These structural data are in line with the docking studies and support the *gauche* effect as being instrumental in inverting the selectivity of enzyme function.

In conclusion, this study reveals that a seemingly subtle 1,3,5-trifluoro bioisostere motif inverts enzyme selectivity relative to the non-fluorinated substrate. Curiously, this change does not inhibit activity, in contrast to the chlorinated analogues. This behaviour has been demonstrated for both the hydrolysis and transesterification to generate all possible stereoisomers. From a translational perspective, and as drug discovery expands into 3D chemical space,[21] clarifying the effect of multiple $C(sp^3)$–H to $C(sp^3)$–F substitutions on enzyme function will become more urgent. Whereas single-point alterations may well be tolerated, such as in *Streptomyces cattleya*,[22] delineating the bioisosteric nature of larger fluorinated arrays requires clarification.[7c] The study also demonstrates the value of simple lipases in accessing optically active, stereochemically complex fluorinated species to modulate the physicochemical properties of bioactive small molecules.

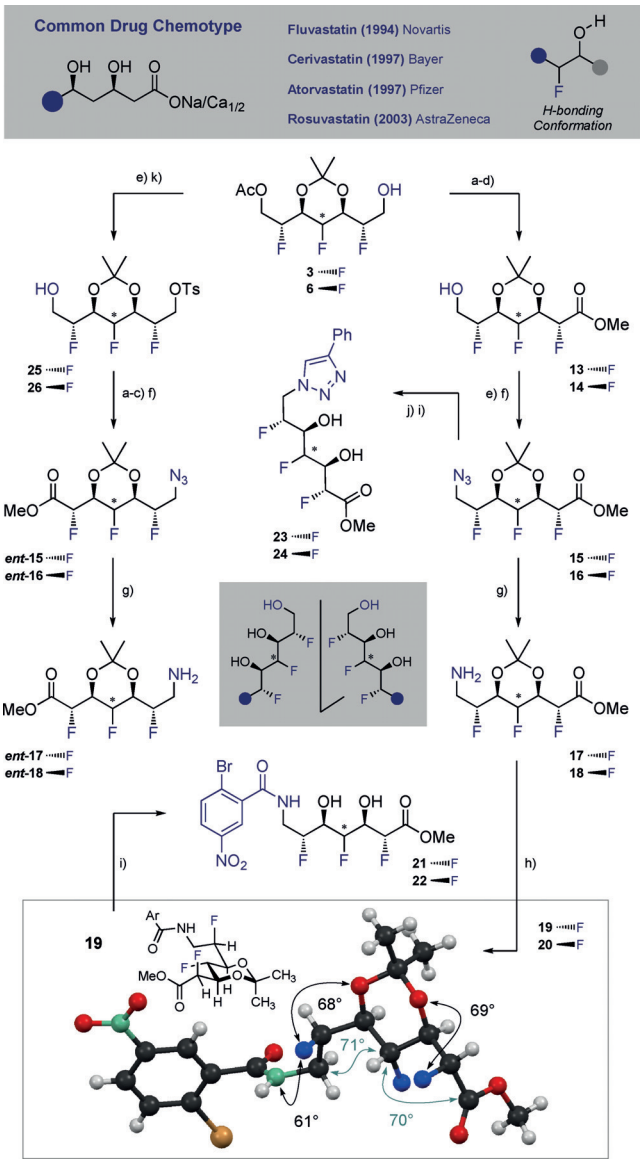

Figure 7. Generation of 1,3,5-trifluoro modified chemotypes common to blockbuster HMG-CoA reductase inhibitors such as Lipitor. a) TEMPO, NaOCl, CH_2Cl_2/H_2O 6:1, 0 °C to rt, 1 h; b) $NaClO_2$, *t*BuOH, 2-methyl-2-butene, phosphate buffer, rt, pH 7, 3 h; c) MeI, $KHCO_3$, DMF, rt, 16 h, **S-21** 70% (3 steps), **S-22** 71% (3 steps), ***ent*-S-23** 86% (3 steps), ***ent*-S-24** 86% (3 steps); d) NaOMe, MeOH/THF 1:1, 0 °C, 3 h, **13** 90% *d.r.* > 12:1, **14** quant.; e) NEt_3, DMAP, TsCl, CH_2Cl_2, rt, 18 h, **S-23** 90%, **S-24** 65%, **S-25** 91%, **S-26** 94%; f) NaN_3, DMF, 80 °C, 18 h, **15** 70%, **16** 94%, ***ent*-15** 70%, ***ent*-16** 75%; g) Pd/C, H_2, EtOAc, rt, 20 h, **17** quant., **18** quant., ***ent*-17** quant., ***ent*-18** quant.; h) RCOCl, Et_3N, CH_2Cl_2, 16 h, **19** 30%, **20** 45%; i) CH_2Cl_2, TFA, H_2O, 100:10:1, rt, 16 h, **21** 68%, **22** 35%, **23** 85%, **24** 54%; j) phenylacetylene, Na-ascorbate, $CuSO_4 \cdot 5H_2O$, DMF, 50 °C, 16 h, **S-27** 98%, **S-28** 96%; k) KOH, MeOH, rt, 2 h, **25** 80%, **26** quant. Please note that "**S**" refers to substrates described in the Supporting Information.

 © 2019 The Authors. Published by Wiley-VCH Verlag GmbH & Co. KGaA, Weinheim

Acknowledgements

We acknowledge financial support from the WWU Münster, the Deutsche Forschungsgemeinschaft (SFB 858, P.B.), and the Helmholtz-Association's Initiative and Networking Fund. The European Commission is acknowledged for an Intra-European Marie Skłodowska-Curie actions fellowship under Horizon-2020 (796089-NovInDXS, R.P.J.) and an ERC Consolidator Grant (R.G., 818949 RECON ERC-2018-CoG).

Conflict of interest

The authors declare no conflict of interest.

Keywords: biocatalysis · conformation · fluorine · *gauche* effect · molecular recognition

How to cite: *Angew. Chem. Int. Ed.* **2019**, *58*, 10990–10994
Angew. Chem. **2019**, *131*, 11106–11110

[1] a) A. Eschenmoser, L. Ruzicka, O. Jeger, D. Arigoni, *Helv. Chim. Acta* **1955**, *38*, 1890–1904; b) A. Eschenmoser, D. Arigoni, *Helv. Chim. Acta* **2005**, *88*, 3011–3048.
[2] J. W. Cornforth, *Pure Appl. Chem.* **1961**, *2*, 607–630.
[3] K. C. Nicolaou, E. J. Sorensen, *Classics in Total Synthesis*, Wiley-VCH, Weinheim, **1996**; K. C. Nicolaou, S. A. Snyder, *Classics in Total Synthesis II*, Wiley-VCH, Weinheim, **2003**.
[4] G. Stork, A. W. Burgstahler, *J. Am. Chem. Soc.* **1955**, *77*, 5068–5077.
[5] For excellent reviews of acyclic conformational analysis, see a) R. W. Hoffmann, *Angew. Chem. Int. Ed. Engl.* **1992**, *31*, 1124–1134; *Angew. Chem.* **1992**, *104*, 1147–1157; b) R. W. Hoffmann, *Angew. Chem. Int. Ed.* **2000**, *39*, 2054–2070; *Angew. Chem.* **2000**, *112*, 2134–2150.
[6] a) K. Müller, C. Faeh, F. Diederich, *Science* **2007**, *317*, 1881–1886; b) M. Salwiczek, E. K. Nyakatura, U. I. M. Gerling, S. Ye, B. Koksch, *Chem. Soc. Rev.* **2012**, *41*, 2135–2171; c) E. P. Gillis, K. J. Eastman, M. D. Hill, D. J. Donnelly, N. A. Meanwell, *J. Med. Chem.* **2015**, *58*, 8315–8359; d) A. Harsanyi, G. Sandford, *Green Chem.* **2015**, *17*, 2081–2086.
[7] a) Q. A. Huchet, B. Kuhn, B. Wagner, N. A. Kratochwil, H. Fischer, M. Kansy, D. Zimmerli, E. M. Carreira, K. Müller, *J. Med. Chem.* **2015**, *58*, 9041–9060; b) I. G. Molnár, C. Thiehoff, M. C. Holland, R. Gilmour, *ACS Catal.* **2016**, *6*, 7167–7173; c) N. A. Meanwell, *J. Med. Chem.* **2018**, *61*, 5822–5880; d) N. Erdeljac, G. Kehr, M. Ahlqvist, L. Knerr, R. Gilmour, *Chem. Commun.* **2018**, *54*, 12002–12005.
[8] D. B. Berkowitz, K. R. Karukurichi, R. de la Salud-Bea, D. L. Nelson, C. D. McCune, *J. Fluorine Chem.* **2008**, *129*, 731–742.
[9] a) L. E. Zimmer, C. Sparr, R. Gilmour, *Angew. Chem. Int. Ed.* **2011**, *50*, 11860–11871; *Angew. Chem.* **2011**, *123*, 12062–12074; b) F. Scheidt, P. Selter, N. Santschi, M. C. Holland, D. V. Dudenko, C. Daniliuc, C. Mück-Lichtenfeld, M. R. Hansen, R. Gilmour, *Chem. Eur. J.* **2017**, *23*, 6142–6149.
[10] a) D. O'Hagan, *Chem. Soc. Rev.* **2008**, *37*, 308–319; b) C. Thiehoff, Y. P. Rey, R. Gilmour, *Isr. J. Chem.* **2017**, *57*, 92–100; c) M. Aufiero, R. Gilmour, *Acc. Chem. Res.* **2018**, *51*, 1701–1710.
[11] For direct, catalytic approaches to generate this motif see: a) S. M. Banik, J. W. Medley, E. N. Jacobsen, *J. Am. Chem. Soc.* **2016**, *138*, 5000–5003; b) I. G. Molnár, R. Gilmour, *J. Am. Chem. Soc.* **2016**, *138*, 5004–5007; c) F. Scheidt, M. Schäfer, J. C. Sarie, C. G. Daniliuc, J. J. Molloy, R. Gilmour, *Angew. Chem. Int. Ed.* **2018**, *57*, 16431–16435; *Angew. Chem.* **2018**, *130*, 16669–16673; d) M. K. Haj, S. M. Banik, E. N. Jacobsen, *Org. Lett.* **2019**, https://doi.org/10.1021/acs.orglett.9b00938.
[12] For an example of a surprisingly high level of discrimination for F-acetyl-CoA versus acetyl-CoA (i.e. single F versus H), see: a) A. W. Weeks, M. C. Y. Chang, *Proc. Natl. Acad. Sci. USA* **2012**, *109*, 19667–19672; b) A. M. Weeks, N. S. Keddie, R. D. P. Wadoux, D. O'Hagan, M. C. Y. Chang, *Biochemistry* **2014**, *53*, 2053–2063.
[13] C. Bonini, R. Racioppi, L. Viggiani, G. Righi, L. Rossi, *Tetrahedron: Asymmetry* **1993**, *4*, 793–805.
[14] For an application in the synthesis of the C1–C13 fragment of amphotericin B, see C. Bonini, L. Chiummiento, A. Martuscelli, L. Viggiani, *Tetrahedron: Asymmetry* **2004**, *45*, 2177–2179.
[15] For selected examples of stereochemically rich fluoroalkanes, see a) D. Farran, A. M. Z. Slawin, P. Kirsch, D. O'Hagan, *J. Org. Chem.* **2009**, *74*, 7168–7171; b) L. Hunter, A. M. Z. Slawin, P. Kirsch, D. O'Hagan, *Angew. Chem. Int. Ed.* **2007**, *46*, 7887–7890; *Angew. Chem.* **2007**, *119*, 8033–8036; c) D. O'Hagan, *J. Org. Chem.* **2012**, *77*, 3689–3699.
[16] a) B. D. Roth, *Prog. Med. Chem.* **2008**, *40*, 1–22; b) B. D. Roth, C. J. Blankley, A. W. Chucholowski, E. Ferguson, M. L. Hoefle, D. F. Ortwine, R. S. Newton, C. S. Sekerke, D. R. Sliskovic, M. Wilson, *J. Med. Chem.* **1991**, *34*, 357–366; c) L. Tabernero, D. A. Bochar, V. W. Rodwell, C. V. Stauffacher, *Proc. Natl. Acad. Sci. USA* **1999**, *96*, 7167–7171; d) E. S. Istvan, J. Deisenhofer, *Science* **2001**, *292*, 1160–1164; e) M. Müller, *Angew. Chem. Int. Ed.* **2005**, *44*, 362–365; *Angew. Chem.* **2005**, *117*, 366–369; f) H. Yasukouchi, K. Machida, A. Nishiyama, M. Mitsuda, *Org. Process Res. Dev.* **2019**, *23*, 654–659.
[17] S. Fischer, N. Huwyler, S. Wolfrum, E. M. Carreira, *Angew. Chem. Int. Ed.* **2016**, *55*, 2555–2558; *Angew. Chem.* **2016**, *128*, 2601–2604.
[18] PyMol-Schrödinger: The PyMOL Molecular Graphics System, Version 1.8 Schrödinger, LLC.
[19] a) BioSolveIT GmbH, Sankt Augustin. http://www.biosolveit.de, LeadIT, version 2.3.2; b) BioSolveIT GmbH, Sankt Augustin. http://www.biosolveit.de, SeeSAR, version 8.1.
[20] For an example of a mono-fluorinated analogue of this drug chemotype, see J. Saadi, H. Wennemers, *Nat. Chem.* **2016**, *8*, 276–280.
[21] F. Lovering, J. Bikker, C. Humblet, *J. Med. Chem.* **2009**, *52*, 6752–6756; F. Lovering, *MedChemComm* **2013**, *4*, 515–519.
[22] a) D. O'Hagan, C. Schaffrath, S. L. Cobb, J. T. Hamilton, C. D. Murphy, *Nature* **2002**, *416*, 279; b) C. Dong, F. Huang, H. Deng, C. Schaffrath, J. B. Spencer, D. O'Hagan, J. D. Naismith, *Nature* **2004**, *427*, 561–565.

Manuscript received: May 2, 2019
Revised manuscript received: May 31, 2019
Accepted manuscript online: June 3, 2019
Version of record online: July 3, 2019

 © 2019 The Authors. Published by Wiley-VCH Verlag GmbH & Co. KGaA, Weinheim